Ultra-Low-Cost Passive 3D-Printed Vibration Transducers for Condition Monitoring by means of Wireless Chipless Transponders

Valentina Palazzi[#1], Paolo Mezzanotte[#], Federico Alimenti[#], Manos Tentzeris[$], Luca Roselli[#]
[#]Department of Engineering, University of Perugia, Perugia, Italy
[$]School of Electrical and Computer Engineering, Georgia Insitute of Technology, Atlanta, GA, USA
[1]valentina.palazzi@unipg.it

***Abstract* — This paper presents a novel displacement transducer, based on a 3-dimensional coupled-line directional coupler, suitable for wireless passive vibration sensing. The 3-D printed transducer is based on two quarter-wave microstrip lines, which are aligned one on top of the other so that part of the signal flowing in one line is coupled to the other. The four ports of the directional coupler are realized on the same layer by adopting two transmission-line transitions. The circuit is manufactured with stereolithography 3-D printing. Selective metallization is achieved by embossing the desired patterns on the 3-D printed dielectric and then applying silver nanoparticle ink to the protruding areas. Vibrations change the distance between the lines, thereby modulating the coupling coefficient of the directional coupler. This way, the sensed vibration can be encoded in the amplitude modulation (AM) of a backscattered RF carrier. This information can be transmitted in real time and recovered by the reader using a simple AM demodulator without the need for any additional electronic component on the tag, that, thus, results in an ultra-low-cost chipless sensor.**

***Keywords* — 3-D printing, additive manufacturing, back-scatter modulation, chipless sensor, condition monitoring, directional coupler, Internet of Things, stereolithography, transmission-line transition, vibration sensor**

I. INTRODUCTION

Over the last decade 3-D printing has attracted an increasing attention in circuit manufacturing, for its inherent capability to drastically reduce material waste and manufacturing costs, while providing versatility and fast prototyping [1]- [5]. Enabling the fabrication of complex geometrical structures with various mechanical properties, 3-D printing makes it possible not only to develop original radio-frequency (RF) solutions, but also to explore innovative sensing approaches [6]. Indeed, the possibility to use resins with different tensile modulus, and to readily vary thicknesses and shapes, makes it possible to realize RF circuit components with transmission properties dependent on the applied force. Such behavior can be profitably used to implement vibration transducers.

Vibration sensors are used in many fields, including condition monitoring. Indeed, the spectral analysis of the vibrations of machines can give us information on their status, and help us perform preventive maintenance. Vibration transducers are usually based on MEMS accelerometers, piezoelectric or piezoresistive materials, and fiber optics [7], [8]; the wireless sensors based on these transducers are generally active, requiring periodic battery charging, bulky and expensive, which limits their large-scale deployment [9].

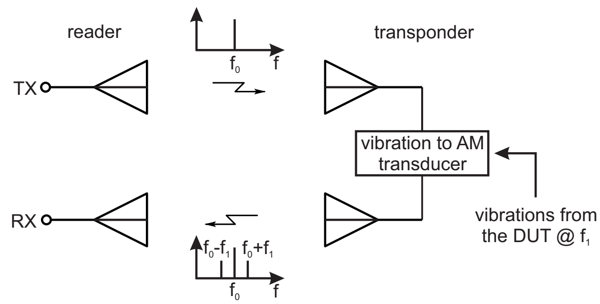

Fig. 1. Schematic representation of the presented sensor.

In this paper a novel vibration transducing approach is developed, based on stereolithography 3-D printing technology, which does not require any piezo-electric or piezo-resistive material. The paper is organized as follows: Sec. II illustrates the detailed design procedure of the transducer, Sec. III focuses on the adopted manufacturing technology. Then, the experimental results are presented in Sec. IV and, finally, in Sec. V the conclusions are drawn.

II. THEORETICAL ANALYSIS

The working principle of the proposed sensor is shown in Fig. 1. The transponder, attached to the device under test (DUT), is interrogated with a sinusoidal signal at f_0. The DUT can be a vibrating platform, such as an aircraft, or an industrial machinery. If no vibrations occur, the transponder reflects the signal, without changing its spectrum. If the DUT undergoes vibrations, instead, the sensor leverages the dynamic displacement caused by the vibrations to modulate the f_0 carrier. This way, the vibration amplitude and frequency are encoded in sidebands and can be retrieved by the reader.

The novelty of the paper lies in the fact that the transducer, based on a 3-D printed RF component, is passive and does not require any non-linear or piezo-electric component. It consists of a 3-D coupled-line directional coupler, where the distance between lines varies when a force is applied.

The layout of the presented topology is shown in Fig. 2. The core of the transducer consists of two $50\,\Omega$ lines in microstrip technology, facing each other according to the following stackup: ground plane - dielectric - strip - air - strip - dielectric - ground plane, as shown in Fig. 2(b). Due to the close proximity of the strips part of the electric field couples from one line to the other. The thickness of the composite microstrip substrate for each layer is $h_1 + h_2$ (see Sec. III). The length of the coupled lines (denoted with "l_c" in Fig. 2(a))

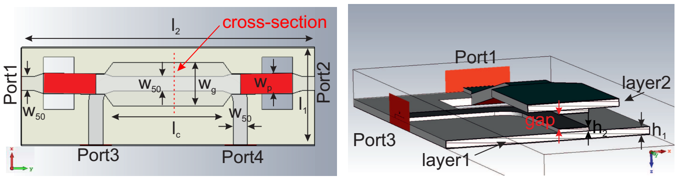

(a) (b)

Fig. 2. Circuit layout: (a) top view and (b) cross-section. The main parameters are: $w_{50} = 3.3$ mm, $w_p = 4.6$ mm, $w_g = 10$ mm, $l_1 = 21.8$ mm, $l_2 = 67$ mm, $l_c = 29$ mm, $h_1 = 0.85$ mm, $h_2 = 0.4$ mm, and $gap = 1.5$ mm.

is $\lambda/4$, where λ is the guided wavelength at the operating RF carrier frequency of the circuit. That way, the circuit operates as a directional coupler (i.e., if Port1 is the input port, then Port2 is the direct port, Port3 is the isolated port, and Port4 is the coupled port, according to the numbering reported in Fig. 2(a)). For demonstration purposes the circuit is designed to operate using an RF carrier of 2.6 GHz.

All four ports, in microstrip technology, are matched to $50\,\Omega$, and are realized on the same layer (layer1), so that the transducer can be interfaced with a planar circuit. To make this possible, two transmission-line transitions are utilized at both ends of the microstrip line on layer2. In particular, the following transitions are implemented: microstrip to parallel plate, and parallel plate to microstrip, where each plate of the parallel plate waveguide transitions into the strip at one end and into the ground plane at the other end, as shown in Fig. 2(a), denoting the parallel-plate waveguides in red.

The parallel plate waveguides, therefore, connect layer1, which is the layer attached to the DUT, and used to interface the transducer with the rest of the circuitry, to layer2, which is suspended, and have the appropriate dimensions to feature a characteristic impedance Z_0 of $50\,\Omega$, as follows:

$$Z_0 = \frac{\eta h_p}{w_p}, \tag{1}$$

where η is the intrinsic impedance of the substrate, h_p is the distance between the parallel plates, equal to $h_1 + h_2$ in the present case, and w_p is the plate width. Two rectangular apertures are realized on the ground plane of layer1 to allow for the connection between the parallel plate waveguides and the circuit ports in microstrip technology.

If the distance between the two strips (indicated with "gap" in Fig. 2(b)) is modified through an applied force, the coupling between Port1 and Port4 also varies accordingly, thereby changing the amount of power that flows from one line to the other.

Let $V_1 = \cos(2\pi f_0 t)$ be the normalized input signal at Port1. If no force is applied, the signal coupled to Port 4 is

$$V_4^0 = C\,V_1, \tag{2}$$

where C is the voltage coupling coefficient between Port1 and Port4. If a vibration is applied, so that the distance between the two lines varies periodically, the output signal is modulated in amplitude as follows (a first order approximation is adopted, corresponding to the case of a sinusoidal vibration):

$$V_4 = C[1 + m\cos(2\pi f_1 t)]V_1, \tag{3}$$

where f_1 is the vibration frequency and m is the modulation index, which depends on the maximum displacement between the two lines. Expanding (3) we obtain:

$$V_4 = C\{V_1 + \frac{m}{2}\cos[2\pi(f_0 + f_1)t] + \frac{m}{2}\cos[2\pi(f_0 - f_1)t]\}. \tag{4}$$

Equation (4) clearly demonstrates that vibrations cause sidebands at the sum and difference frequencies, and that information on the vibration characteristics can be retrieved from the amplitude and frequency of these signals.

Due to its geometrical complexity, the presented structure cannot be realized with traditional technologies, but it is suitable for low-cost 3-D printing. Moreover, the transducer can be easily integrated in a wireless transponder by connecting Port1 and Port4 to two antennas, as shown in Fig. 1, and information can be transferred by backscatter modulation.

III. Prototyping

A proof-of-concept prototype for the above sensor is realized with additive technologies. The dielectric scaffolding was manufactured using stereolithography 3D printing. According to this technology, liquid photoreactive resins are laser-cured, to yield solid objects with arbitrary shapes. In particular, the "clear" photoreactive resin from FormLab and the Form 2 printer were chosen, as they combine low cost with the possibility to achieve a satisfactory resolution for RF circuits (i.e., up to $25\,\mu$m). The resin was electromagnetically characterized in the frequency range of interest, where it shows a dielectric constant ϵ_r of 2.8 and a $\tan\delta$ of 0.03 [4] .

Metallization, instead, was performed applying silver nanoparticle ink from Suntronic to the 3D printed surface with a brush for laboratory validation. Selectivity was achieved adopting the embossed-surface patterning technique described in [4]. The areas corresponding to the strips, which were destined for ink deposition, were extruded in a protruded fashion with respect to the rest of the surface (the step height is indicated with "h_2" in Fig. 2(b)). The brush bristles were applied parallel to the embossed parts, so that unwanted surface was not touched. After each ink deposition, the sample was cured at $110\,^\circ$C for 10 minutes, to let solvents evaporate, and 4/5 layers of ink were applied to achieve a metallization thickness of about $10\,\mu$m and a conductivity of about 1×10^6 S/m.

Fig. 3 shows the fabricated prototype at different stages. The initial distance "gap" between lines was chosen to obtain a coupling of about -20 dB in the band of interest, corresponding to 1.2 mm. Fig. 3(a) shows the dielectric scaffolding after printed supports and excess liquid resin were removed. With respect to the model shown in Fig. 2, layer2 was slightly curved to ease the access of the brush to the coupled lines. Layer1 is a flat object with very high aspect ratio. Its thickness uniformity is therefore a critical parameter.

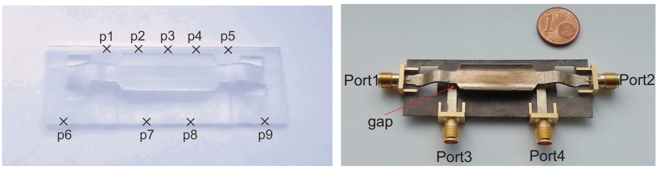

(a) (b)

Fig. 3. Circuit prototype: (a) dielectric scaffolding and (b) complete prototype.

Fig. 4. Experimental setup.

The substrate thickness "h_1" was sampled at different points (marked with a cross in Fig. 3(a)) with a digital caliper. A thickness error lower than 6% was observed.

Fig. 3(b) shows the complete prototype after metallization. The transducer consists of a single piece and weighs 2 grams. End-launch SMA connectors were attached to the ports of the circuit with a colloidal silver paste for measurement purposes.

IV. Experimental Results

The experimental setup in Fig. 4 is used to validate the presented vibration transducer. The prototype is placed in contact with a shaker (model DS-PM-20 from DEWESoft). Port1 is connected to an RF signal generator at 2.6 GHz (the transmitted power is 0 dBm for the purpose of testing). Port4 is connected to a spectrum analyzer (measurement band: 3 KHz centered at 2.6 GHz, resolution bandwidth: 5 Hz). Port2 and Port3 are terminated to matched loads.

Fig. 5 shows the signal acquired by the spectrum analyzer with and without vibrations. When the shaker is switched off, the measured spectrum corresponds to the spectrum of the RF transmitted signal, attenuated by the coupling coefficient C of the 3-D directional coupler (see Fig. 5(a)). When the shaker is switched on, instead, sidebands appear at the frequencies $f_0 \pm n f_1$, where n is a positive integer, as shown in Fig. 5(b). The harmonic components depend on the actual mechanical wave applied by the shaker, which is different from a simple sinusoid. In the reported experiment the vibration frequency was chosen to be $f_1 = 500$ Hz, and the gain knob of the shaker is set to its maximum value. The sideband components are 25.6 dB below the carrier, corresponding to a modulation index m of 10.5%.

In Fig. 6(a) the power of the RF carrier is varied. The frequency of the sidebands is the same regardless of the carrier power level, while their magnitude scales by the same amount as the carrier. Therefore, the modulation index m does not depend on the carrier power, but only on the vibration amplitude, meaning that the information acquired by the complete wireless sensor can be recovered regardless of the tag-to-reader distance. Finally, a reference accelerometer (model ADXL354 from Analog Devices) is used to evaluate the transducer performance versus acceleration. In the preliminary study shown in Fig. 6(b), a variation in the sideband amplitude of 10 dB is observed for an acceleration varying from 0.5 g to 1 g.

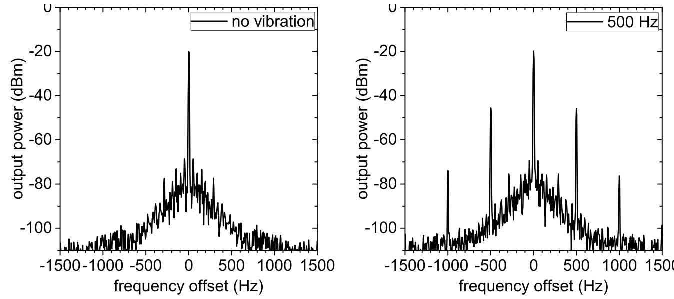

(a) (b)

Fig. 5. Frequency domain response of the proposed transducer (a) without vibrations, and (b) with a 500 Hz vibration.

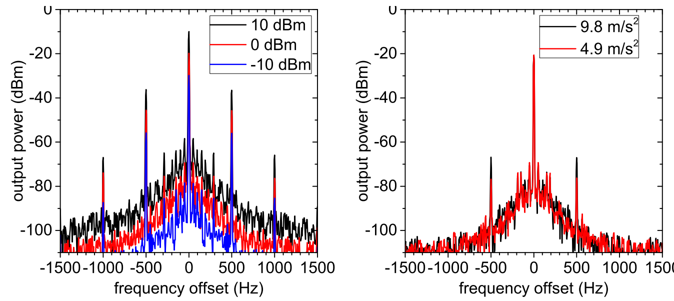

(a) (b)

Fig. 6. Transducer characterization: frequency domain response (a) for various carrier power levels, and (b) for various acceleration values.

V. Conclusion

A novel 3D-printed passive transducer for wireless vibration sensing has been presented. The transducer is based on a 3-D directional coupler, where the lines are aligned one on top of the other on two different layers. That way, the line distance can be varied by an applied force, causing the amplitude modulation of the coupling coefficient. A proof-of-concept prototype has been manufactured and experimentally validated. The transducer succeeded in detecting a vibration with a frequency of 500 Hz, for variable carrier powers and accelerations. Leveraging the capability of 3-D printing to manufacture complex dielectric shapes, the transducer sensitivity can be readily tuned, by changing the curvature of the two parallel-plate waveguides used to connect layer 1 to layer 2, and the layer thickness. The proposed transduction approach can be used for extremely low-cost wireless passive sensing, as vibrations can be encoded in the amplitude modulation of a backscattered RF carrier without using any chip, thereby making it an excellent ultra-low-cost candidate for condition monitoring applications.

References

[1] J. Maas, B. Liu, S. Hajela, Y. Huang, X. Gong, and W. J. Chappell, "Laser-Based Layer-by-Layer Polymer Stereolithography for

High-Frequency Applications," *Proc. IEEE*, vol. 105, no. 4, pp. 645–654, Apr. 2017.

[2] A. I. Dimitriadis, T. Debogovic, M. Favre, M. Billod, L. Barloggio, J.-P. Ansermet, and E. de Rijk, "Polymer-Based Additive Manufacturing of High-Performance Waveguide and Antenna Components," *Proc. IEEE*, vol. 105, no. 4, pp. 668–676, Apr. 2017.

[3] R. Bahr, B. Tehrani, and M. M. Tentzeris, "Exploring 3-D Printing for New Applications: Novel Inkjet- and 3-D-Printed Millimeter-Wave Components, Interconnects, and Systems," *IEEE Microw. Mag.*, vol. 19, no. 1, pp. 57–66, Jan. 2018.

[4] V. Palazzi, W. Su, R. Bahr, S. Bittolo-Bon, F. Alimenti, P. Mezzanotte, L. Valentini, M. M. Tentzeris, and L. Roselli, "3-D-Printing-Based Selective-Ink-Deposition Technique Enabling Complex Antenna and RF Structures for 5G Applications up to 6 GHz," *IEEE Trans. Compon. Packag. Manuf. Technol.*, vol. 9, no. 7, pp. 1434–1447, Jul. 2019.

[5] V. Palazzi, A. Cicioni, F. Alimenti, P. Mezzanotte, M. M. Tentzeris, and L. Roselli, "Compact 3-D-Printed 4 x 4 Butler Matrix Based on Low-Cost and Curing-Free Additive Manufacturing," *IEEE Microw. Wireless Compon. Lett.*, vol. 31, no. 2, pp. 125–128, Feb. 2021.

[6] M. R. Khosravani and T. Reinicke, "3D-printed sensors: Current progress and future challenges," *Sensors and Actuators A: Physical*, vol. 305, p. 111916, Apr. 2020.

[7] Z. T. Nishino, K. Chen, and N. Gupta, "Power Modulation-Based Optical Sensor for High-Sensitivity Vibration Measurements," *IEEE Sensors J.*, vol. 14, no. 7, pp. 2153–2158, Jul. 2014.

[8] A. Sabato, C. Niezrecki, and G. Fortino, "Wireless MEMS-Based Accelerometer Sensor Boards for Structural Vibration Monitoring: A Review," *IEEE Sensors J.*, vol. 17, no. 2, pp. 226–235, Jan. 2017.

[9] PCE Intruments UK, "Condition Monitoring Wireless Vibration Monitor PCE-VMS 504." [Online]. Available: https://www.pce-instruments.com/english/measuring-instruments/test-meters/condition-monitoring-pce-instruments-condition-monitoring-wireless-vibration-monitor-pce-vms-504-det_1051935.htm